Check for updates



www.chemeurj.org

Structural Impact of N-terminal Pyroglutamate in an Amyloid- β (3-42) Fibril Probed by Solid-State NMR Spectroscopy

Luis Gardon⁺, [a, b] Nina Becker⁺, [a, b] Lothar Gremer, *[a, b] and Henrike Heise*[a, b]

Extracellular amyloid- β (A β) plaques, primarily formed by A β (1-40) and A β (1-42) fibrils, are a hallmark of Alzheimer's disease. The A β peptide can undergo a high variety of different post-translational modifications including formation of a pyroglutamate (pGlu, pE) at N-terminal Glu3 or Glu11 of truncated A β (3-x) or A β (11-x), respectively. Here we studied structural similarities and differences between pEA β (3-42) and LS-shaped A β (1-42) fibrils grown under identical conditions (pH 2) using solid-

state NMR spectroscopy. We show that the central region of pEA β (3-42) fibrils including the turn region around V24 is almost identical to A β (1-42) showing similar β -strands also at the N-terminus. The missing N-terminal residues D1-A2 along with pE3 formation in pEA β (3-42) preclude a salt bridge between K28-D1' as in A β (1-42) fibrils. G37 and G38 act as highly sensitive internal sensors for the modified N-terminus, which remains rigid over ~five pH units.

Introduction

Aggregation of amyloid- β (A β) is closely linked to Alzheimer's disease (AD). The dominant components of the senile A β plaques are A β (1-40) and A β (1-42), the latter has been shown to be more aggregation prone and more toxic. In addition to the full-length peptides, different N- and C-terminally truncated A β species (e.g. 3-x, 11-x), as well as various post-translational modifications are found in the plaques of AD patients and were shown to have altered biological and biophysical properties. N-terminal Glu residues in truncated A β (3-x) or A β (11-x) are usually converted to a cyclic pyroglutamate residue (pyroGlu, pE) (Figure 1A) catalyzed by glutaminyl cyclases, QC, Ial leading to pE-modified A β species (pEA β).

Compared to A β (1-42), pEA β (3-42) shows higher toxicity in mouse models,^[5] a faster aggregation rate, and it cross seeds and accelerates the aggregation of A β (1-42).^[6] NMR studies on monomeric pEA β (3-40) and pEA β (3-42) revealed significant

В glutamine pEAβ(3-42) Aβ(E3Q-42) 19 20 16 17 18 H_2N Time (min) -0 h -24 h C 10.0 nm pH 3.5 OC or QC catalyzed catalyzed H_2O NH₄ pyroglutamate

Figure 1. Production and detection of pEAβ(3-42) fibrils. A) Scheme of pyroglutamylation of Aβ(3-42) or Aβ(E3Q-42) to pEAβ(3-42), and B) analysis by RP-HPLC. HPLC runs are shown after 0 h (black) and 24 h (blue) incubation time at pH 3.5. pEAβ(3-42) is already visible at time 0 h since its formation already starts during TEV cleavage of the fusion construct. C) AFM image of pEAβ(3-42) fibrils.

[a] L. Gardon, N. Becker, L. Gremer, H. Heise
 Institute of Biological Information Processing (IBI-7: Structural Biochemistry) and JuStruct: Jülich Center for Structural Biology
 Forschungszentrum Jülich
 52425 Jülich, Germany

E-mail: l.gremer@fz-juelich.de h.heise@fz-juelich.de

[b] L. Gardon,* N. Becker,* L. Gremer, H. Heise Physikalische Biologie Heinrich-Heine-Universität Düsseldorf 40225 Düsseldorf, Germany

[+] sharing 1st authorship

Supporting information for this article is available on the WWW under https://doi.org/10.1002/chem.202303007

© 2023 The Authors. Chemistry - A European Journal published by Wiley-VCH GmbH. This is an open access article under the terms of the Creative Commons Attribution Non-Commercial NoDerivs License, which permits use and distribution in any medium, provided the original work is properly cited, the use is non-commercial and no modifications or adaptations are made.

chemical shift perturbations for the N-terminal residues up to G9, while the rest of the sequence remains relatively unperturbed compared to A β (1-40) and A β (1-42), respectively. In contrast to pEA β (3-42) fibrils, pEA β (3-40) fibrils and pEA β (11-40) fibrils have already been well characterized by solid-state NMR and revealed only small structural changes limited to the N-terminus when compared to A β (1-40) fibrils. The N-terminus is, however, flexible in the systems studied. Different to *in vitro* A β (1-42) fibril structures with flexible N-termini, an LS-shaped A β (1-42) fibril morph with the entire N-terminus being part of the rigid core can be produced at pH 2 in 30% acetonitrile, and its atomic structure was determined in a combined cryo-EM/ solid-state NMR study. In State NMR study.

These fibrils retained their structure including the fixed rigid N-terminus, apart from few salt bridge rearrangements, when

exposed to pH 7.^[11] Here, we used identical fibril preparation conditions^[10-11] for recombinant pEA β (3-42), report on a complete NMR resonance assignment and secondary structure analysis of pEA β (3-42) fibrils including the influence of a subsequent shift from pH 2 to pH 6.5 and compare it to the structure of LS-shaped A β (1-42) fibrils.

Results and Discussion

For recombinant production of uniformly $[U^{-13}C,^{15}N]$ -labeled pEA β (3-42) we used an A β (E3Q-42) construct because an N-terminal Gln, in contrast to Glu, is able to convert chemically at acidic pH (3.5) into pE (Figure 1A) without the need of a QC catalyst. PEA β (3-42) formation was monitored by RP-HPLC (Figure 1B). pEA β (3-42) has a longer retention time than A β (EQ3-42) due to the lack of the hydrophilic amino group at the N-terminus (Figure 1A). Fibril growth of purified pEA β (3-42) was completed after several weeks under quiescent conditions at room temperature. Mostly nonbranched fibrils without any amorphous aggregates were obtained, as obvious from atomic force microscopy (AFM) (Figure 1C). Far-UV CD spectra of both

pEA β (3-42) fibrils and LS-shaped A β (1-42) fibrils show same characteristics for β -sheet dominated structures (Figure S1).

We compared 2D Proton Driven Spin Diffusion (PDSD) $^{13}C^{-13}C$ fingerprint spectra of A β (1-42) and pEA β (3-42) fibrils (Figure 2A, Table S1). Both spectra show clear similarities, particularly for the range Y10 to I32. Of note, chemical shifts of V24 located in the turn region of A β (1-42) fibrils are highly similar for pEA β (3-42) fibrils (Figure 2A, C). These shifts are characteristic as they show a relatively low C α chemical shift and two distinct C γ resonances typical for steric restriction, which were not observed in the spectra of other A β (1-42) fibril polymorphs with flexible N-termini. Furthermore, both fibrils show identical resonances for S26 and K28 in the PDSD spectra (Figure 2A).

As the two spectra show distinct differences for several amino acids located in other regions (e.g. the N-terminus, G37 and G38, detailed below), we performed a *de novo* resonance assignment for pEA β (3-42) fibrils. Using a combination of different 2D and 3D 13 C- 13 C and NCACX/NCOCX spectra, we assigned all residues unambiguously, except H14, which was not visible (Figure 2E, S2–S4, Table S2). As for LS-shaped A β (1-42) fibrils, [10-11] no protein signals are observed in Insensitive Nuclei Enhancement by Polarization Transfer (INEPT) spectra of

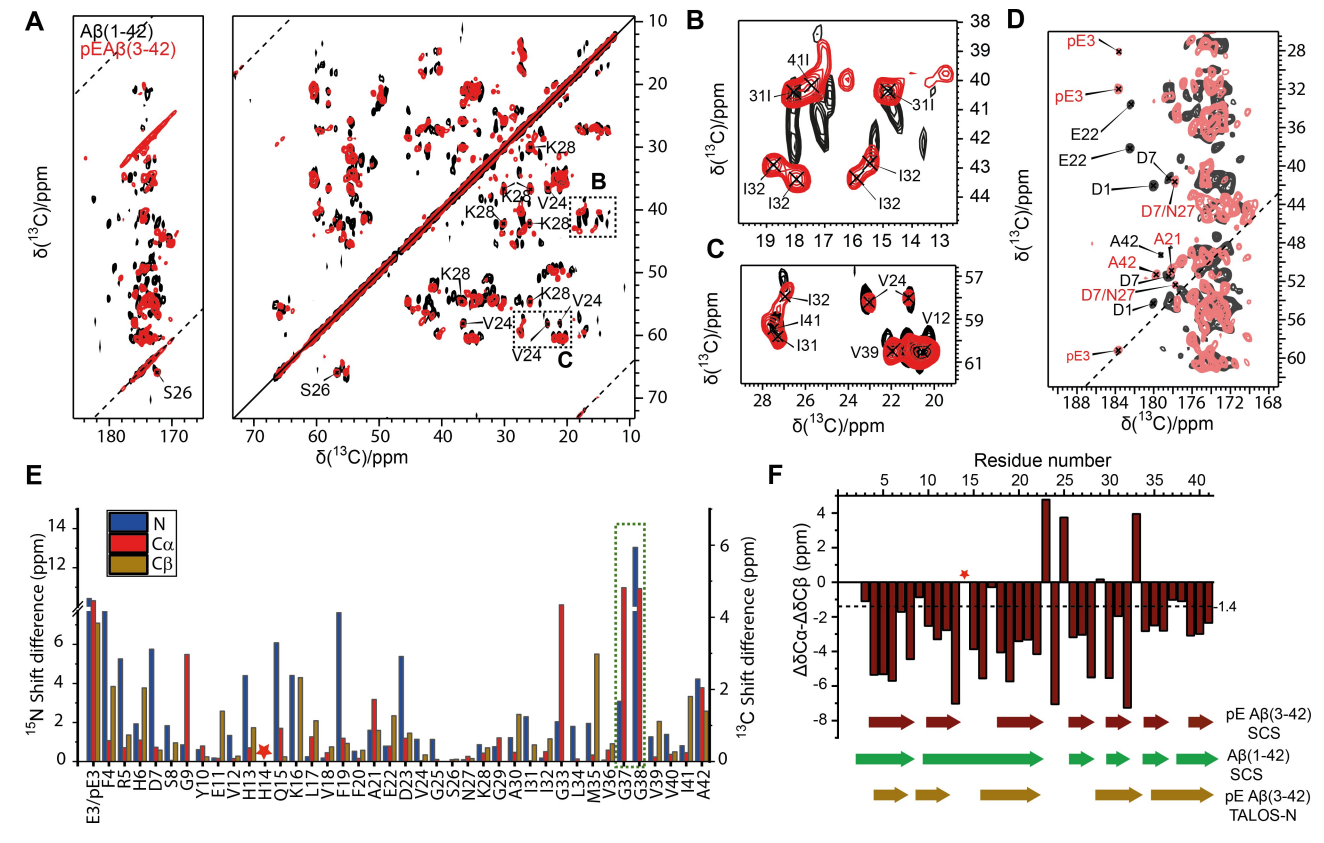


Figure 2. Comparison of pEAβ(3-42) and Aβ(1-42) fibrils produced under identical conditions. A) Overlay of 2D 13 C- 13 C PDSD spectra with 20 ms mixing time at 11 kHz Magic Angle Spinning (MAS) frequency: pEAβ(3-42) fibrils (red) and LS-shaped Aβ(1-42) fibrils (black). ^[10-11] The complete assignment of pEAβ(3-42) fibrils is shown in Figures S2-S4. B, C) Zoomed regions from A: Cβ and Cγ/Cδ cross peaks for lle residues (B) and Cα and Cγ cross peaks for Val (in particular identical V24) and lle residues (C). D) CO-region of 2D 13 C- 13 C PDSD spectra with 200 ms mixing time and 12.5 kHz MAS frequency of Aβ(1-42) fibrils (black) and 2D 13 C- 13 C DARR with 100 ms mixing time and 20 kHz MAS frequency of pEAβ(3-42) fibrils (bright red). pE3 resonances are clearly visible for the pEAβ(3-42) fibrils, whereas resonances for D1-A2 are missing. E) Chemical shift difference of N, Cα and Cβ chemical shifts for pEAβ(3-42) and Aβ(1-42) fibrils. F) Secondary chemical shifts (SCS) and TALOS-N analysis. A β-strand in SCS is defined when three consecutive residues exhibit (Cα-Cαrc)-(Cβ-Cβrc) <-1.4. ^[12] The asterisk marks missing resonances for H14.

Elbrary.wiley.com/doi/10.1002/chem.202303007 by Forschungszentrum Jülich GmbH Research Center, Wiley Online Library on [21/02/2024]. See the Terms and Conditions (https://onlinelibrary.wiley

conditions) on Wiley Online Library for rules of use; OA articles are governed by the applicable Creative Commons

pEAβ(3-42) fibrils, excluding any highly mobile and flexible parts (Figure S8).[13] The carbonyl region of the 13C-13C correlation spectra (PDSD/ Dipolar Assisted Rotational Resonance (DARR)) exhibits resonances for pE3 (Figure 2D) with chemical shifts typical for N-terminal pE,[14] indicating a rigid N-terminus in pEAβ(3-42) fibrils. Some residues, e.g. S26 (as already reported for $A\beta(1-42)$ fibrils^[10]), as well as some Ala and Ile residues (Figure 2B) show peak doubling, the latter due to conformational sidechain disorder.[15] Peak doubling for G37 and G38 in NCOCX spectra indicates local structural variations for both residues (Figure S3). By comparing the chemical shifts of pEA β (3-42) fibrils with those of A β (1-42) fibrils produced under same conditions,^[10] a conserved region (from V24 to K28) can be observed (Figure 2E). The missing D1-A2 residues and pE3 formation in pEAβ(3-42) fibrils led to changes in chemical shifts at the N-terminus up to G9, but also at the C-terminus starting from position G33 with largest changes for ¹³C chemical shifts of G33, G37 and G38 (Figure 2E). Typically, Gly residues allow more flexibility for the peptide backbone and thus are expected to be more sensitive to structural changes induced by the adjacent modified N-terminus. Indeed, G37 and G38 are most affected by the D1-A2 truncation and pE3 modification. Likewise, the ¹⁵N chemical shift of G38 changed by more than 10 ppm to a low value of 103 ppm (Table S2). In LS-shaped $A\beta(1-42)$ fibrils G37 and G38 are in close contact with A2 and part of the hydrophobic cluster composed of A2, V36, F4, L34, G37 and G38.[10]

Information about torsion angles (Figure S5), secondary structure and position of the β -strands in pEA $\beta(3-42)$ fibrils is obtained from secondary chemical shifts and TALOS-N. A comparison with results obtained for LS-shaped A $\beta(1-42)$ fibrils shows similar positions of β -strands (Figure 2F). Correlation plots which relate residue-specific secondary chemical shifts reported *in vitro* structures structures obtained in this work report larger differences relative to S-shaped fibril structures that the structures of the structures of the structures of the structure of the structures of the structure of the s

In LS-shaped A β (1-42) fibrils, F19 and I31 are in close spatial proximity (Figure 3A), which can be probed by $^{13}C^{-13}C$ spin diffusion at rotational resonance. Cross correlation peaks indicating a contact between I31 C δ and the aromatic F19 residue were observed in PDSD spectra, where the spinning speed of 17.2 kHz was matching the chemical shift difference between aromatic Phe and Ile C δ signals (at 600 MHz ^{1}H frequency) in both, pEA β (3-42) and A β (1-42) fibrils (Figure 3B, Figure S7). This supports the conservation of the turn region comprising residues F19 to I31. Interestingly, chemical shifts of C-terminal residues in LS-shaped A β (1-42) fibrils (at pH 2) changed upon a pH shift to pH $7^{[11]}$ towards those observed in pEA β (3-42) fibrils (at pH 2) (Figure 4 A, B). Especially for ^{15}N and $^{13}C\alpha$ of G38 chemical shift differences reduce from 13.0 and 4.8 ppm to 1.7 and 0.4 ppm, respectively.

For LS–A β (1-42) fibrils shifted to pH 7, the changes at the C-terminus are explained by a rearrangement of the salt bridge from K28-D1' at pH 2 to K28-A42 at pH 7. [11] A salt bridge between K28 and a D1' residue is obviously absent in pEA β (3-42) fibrils. We also studied possible alterations of the pEA β (3-42) fibril structure after pH adjustment to pH 6.5 as performed as

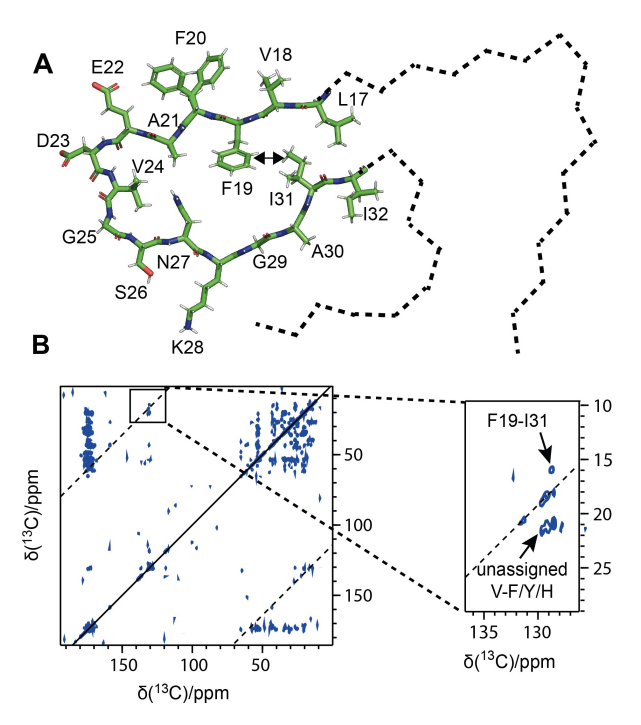


Figure 3. Rotational resonance dipolar recoupling of F19 and I31 sidechains. A) L17 to I32 region of L5-shaped Aβ(1-42) fibrils (PDB:5OQV). ^[10] The turn region includes a close contact between F19 and I31 sidechains. B) PDSD spectra at 17.2 kHz MAS of pEAβ(3-42) fibrils show a cross peak indicating dipolar interaction of an aromatic F19 carbon and I31 Cδ. Cross correlation peaks for V-H/F/Y contacts could not be assigned unambiguously (e.g. V18-F19 or V12-H13).

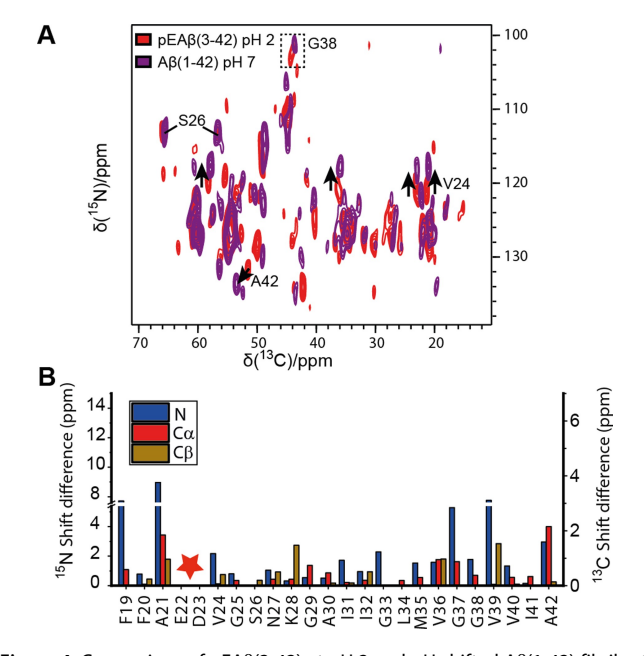


Figure 4. Comparison of pEAβ(3-42) at pH 2 and pH shifted Aβ(1-42) fibrils at pH 7 by addition of citrate-phosphate buffer. A) NCACX spectra at 11 kHz MAS frequency of pEAβ(3-42) at pH 2 and pH shifted Aβ(1-42) fibrils at pH 7.^[11] Resonances for S26 remain unchanged in 13 C and 15 N dimension, for G38 and V24 almost unchanged in 13 C, but shifted in 15 N dimension, for A42 shifted in both dimensions (due to change of its protonation state). Shifts of these resonances are indicated by arrows. B) Chemical shift difference of N, Cα and Cβ chemical shifts for pEAβ(3-42) at pH 2 and pH-shifted Aβ(1-42) fibrils at pH 7. The asterisk marks missing E22/D23 resonance assignments for Aβ(1-42) fibrils at pH 7.

recently described for Aβ(1-42).^[11] The added citrate/phosphate buffer was used as internal pH sensor (Figure S8).

Figure 5A shows the overlay of the 2D ¹³C-¹³C PDSD spectra of pEAβ(3-42) fibrils at pH 2 and pH 6.5. As most of the resonances overlap, we can conclude that the global fold of the pEAβ(3-42) fibrils remains unchanged from pH 2 to pH 6.5. The C-terminal A42 of pEAβ(3-42) fibrils changed from a protonated (at pH 2) to a deprotonated (at pH 6.5) state (Figure 5B), as already observed for LS-shaped Aβ(1-42) fibrils upon a pH shift^[11] with slow proton exchange on the NMR time scale. The fact that A42 is protonated excludes a salt bridge between K28 and A42 at low pH. Strong correlation signals typical for $C\alpha$ - $C\delta$ in deprotonated Glu, likely E22, appear at pH 6.5 (Figure 5B) which is presumably also seen as a shift in the C β -C γ region of E22 (Figure 5D). Likewise, the D7 Cβ resonances shifted by ~2 ppm to higher ppm values (from 41.5 ppm to 43.6 ppm) upon the pH-shift, typical for deprotonation (Figure 5C). For D7 of $A\beta(1-42)$ fibrils a fast proton exchange between the protonated and deprotonated state was observed^[11] which we also assume for pEAβ(3-42) fibrils. No changes are detected for K28, in contrast to pH 7 shifted Aβ(1-42). Compared to our previous work we do not observe any significant intensity losses for pEA β (3-42) fibrils at pH 6.5 as seen for A β (1-42) fibrils at pH 7.^[11]

At pH 6.5 the 1D Direct Excitation (DE) compared to the Cross Polarization (CP) spectra (Figure S8C-D) do not show significant differences, and no INEPT signals were observed. This confirms the absence of any highly mobile parts and further supports a rigid N-terminus also at pH 6.5.

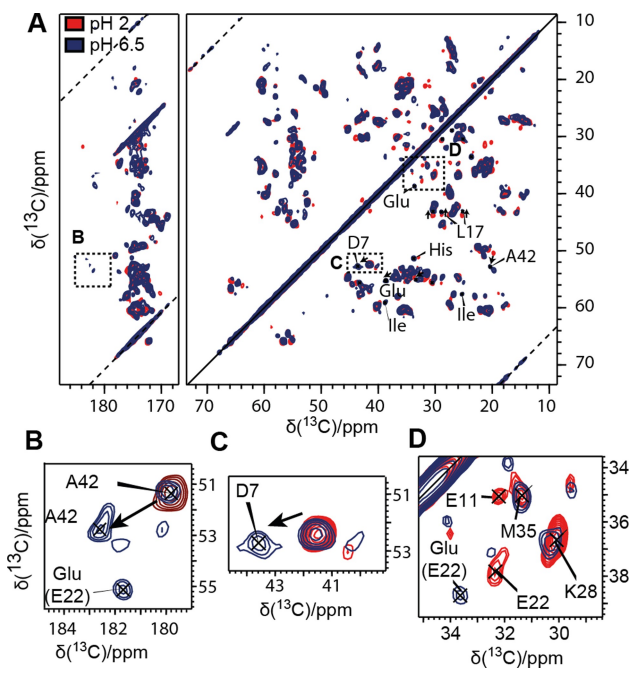


Figure 5. pEAβ(3-42) fibrils at pH 2 and adjusted to pH 6.5. A) Overlay of 2D ³C-¹³C PDSD spectra with 20 ms mixing time of pEAβ(3-42) fibrils at pH 2 (red) and pH 6.5 (navy). B-D) Zoomed regions from A: carbonyl region of A42 for longer mixing time (200 ms) (B) and the shift of the C-terminal A42 indicate a transition from a protonated to a deprotonated state. Cα-Cβ region of D7 (C). C β -C γ region of Glu residues (D).

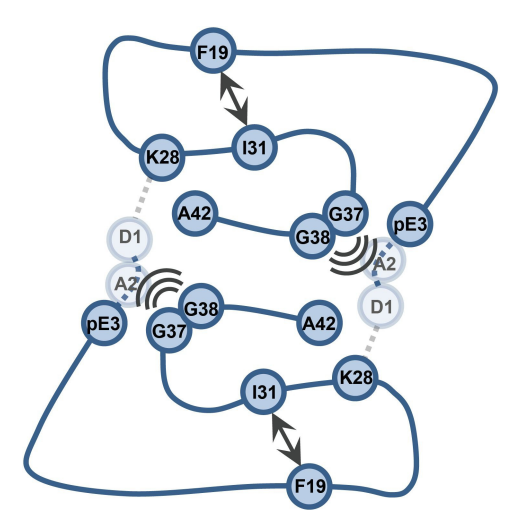


Figure 6. Characteristics of pEA β (3-42) fibrils. The missing N-terminal residues D1-A2 along with pE3 formation in pEAβ(3-42) preclude the formation of a salt bridge between K28-D1'as in $A\beta(1-42)$ fibrils. Residues G37 and G38 sense N-terminal modifications present in pEAB(3-42) fibrils compared to A β (1-42) fibrils. The F19-I31 contact is preserved in both structures.

Water-edited experiments (Figure S9) which probe the global water accessibility also revealed that the overall structure is retained over ~five pH units, as the build-up is only slightly enhanced for pH 6.5 compared to pH 2 due to faster chemical exchange.[11,18]

Conclusions

To conclude, in this study we report an in-depth NMR characterization of a pEA β (3-42) fibril morph at pH 2 and pH 6.5. Comparison with Aβ(1-42) fibrils prepared under identical conditions reveals remarkable structural similarities and indicates a conserved central region spanning residues L17 to I32, around the turn at V24 in both fibrils (Figure 6). The missing Nterminal residues D1-A2 along with pE3 formation in pEAβ(3-42) preclude the formation of a salt bridge between K28-D1' present in A β (1-42) fibrils. Obviously, this salt bridge is not needed for a rigid N-terminus in this fibril morph. G37 and G38 act as highly sensitive sensors for the modified N-terminus as seen by their shift perturbations. Notably, pEA β (3-42) fibrils harbor β-strand positions highly similar to those in LS-shaped $A\beta(1-42)$ fibrils including the rigid N-terminal region.

Experimental Section

Sample preparation

Expression of the His-tagged $A\beta$ (E3Q-42) fusion construct was essentially performed as described^[7a] in 2.5 l cultures of [U-¹³C, ¹⁵N]labeled M9 minimal medium with [U-13C]-glucose and [15N]-NH4CI as sole carbon and nitrogen sources. The medium was inoculated with starter cultures (1:100) and incubated at 37 °C and 120 rpm until an OD₆₀₀ of 0.3 was reached. Protein expression was induced

by adding 0.2 mM isopropyl β -D-1-thiogalactopyranoside (IPTG). The culture was then incubated at 25 °C at 120 rpm overnight. Cells were harvested by centrifugation (5.000 xg, 15 min) and cell pellets were resuspended with ~5 to 8 ml per g cell mass of lysis buffer (50 mM Na phosphate buffer, pH 7.4, 200 mM NaCl, 0.4 mM phenylmethylsulfonyl fluoride (PMSF), 5 mg/ml lysozyme). Cell disrupture was done by sonification under ice cooling (15×10 s on, 60 s off, at 80% amplitude, Bandelin Sonopuls, VS70T sonotrode), and subsequent ultracentrifugation (55.000 xg, 1 h) was used to separate the soluble fraction containing the [U-¹³C, ¹⁵N]-Aβ(E3Q-42) fusion construct from cell debris. Further purification was done by immobilized metal ion affinity chromatography (IMAC). For that the supernatant was loaded on Ni2+-NTA material (two in series connected 5 ml Ni-NTA Protino columns, Macherey-Nagel, Düren, Germany), equilibrated with 50 mM Na phosphate buffer, pH 7.4, 200 mM NaCl, 20 mM imidazole, pH 7.4, and connected to an Äkta prime plus system (Cytiva, Germany). Elution of the fusion construct was achieved by using an imidazole gradient of 20 to 500 mM imidazole in 50 mM Na phosphate buffer, pH 7.4, 200 mM NaCl, using a gradient volume of 87.5 ml at a flow rate of 2.5 ml/min. Subsequently, tobacco etch virus (TEV) protease digestion was performed using 1 mg TEV per 8.5 mg Aβ(E3Q-42) fusion construct in 50 mM Na phosphate buffer, pH 7.4, 200 mM NaCl for 7 days at 4°C. After 3 days incubation 15 mM Tris(2-carboxyethyl)phosphin (TCEP) was added as reducing agent. [U-13C,15N]-Aβ(E3Q-42) was then further purified by semipreparative RP-HPLC on Zorbax SB-300 C8 (9.4 mm x 250 mm column, Agilent, Böblingen, Germany) connected to an Agilent 1260 Infinity system with UV detection at 214 nm and a column temperature of 80 °C. The mobile phase used was isocratic aqueous 30% (v/v) acetonitrile (ACN), 0.1% (v/v) trifluoroacetic acid (TFA). Purified [U-¹³C,¹⁵N]-Aβ(E3Q-42) was freeze dried, and pyroGlu formation of the N-terminal was performed as described^[7a] by dissolving lyophilized [U-¹³C,¹⁵N]-Aβ(E3Q-42) in 30 mM sodium acetate, pH 3.5 (pH adjusted with acetic acid) at a concentration of 0.25 mg/ml and incubation at 4°C for 3 days. A further semipreparative HPLC purification step under the same isocratic conditions (aqueous 30% (v/v) ACN, 0.1% (v/v) TFA, pH 2) as described above yields pure [U-13C,15N]-pEAβ(3-42) with typical purities of above 97%. Fibril growth of pEAβ(3-42) was achieved by quiescent incubation of ~6 μ M pEA β (3-42) directly in the mobile HPLC phase (aqueous 30% (v/v) ACN, 0.1% (v/v) TFA, pH 2) for one month at RT as already described for Aβ(1-42).^[10]

Atomic force microscopy (AFM) and far-UV circular dichroism (CD) spectroscopy

For AFM, typically 4 μ l samples of pEA β (3-42) fibrils in aqueous 30% (v/v) ACN, 0.1% (v/v) TFA, pH 2 at concentrations of 10 to 50 μ M (monomer equivalents) were pipetted on a freshly cleaved mica support and incubated for 10 min. Then the mica was dried with a gas stream of nitrogen. AFM micrographs were recorded in peakforce tapping mode on a Bruker Multimode 8 (Billerica, Massachusetts, USA) using OMCL-AC160TS cantilevers (Shinjuku, Tokyo, Japan) using ScanAsyst software at 1024x1024 pixel resolution. The images were processed with Gwyddion 2.61. [19]

For far-UV CD spectroscopy, samples of pEA β (3-42) fibrils or A β (1-42) fibrils in aqueous 30% (v/v) ACN, 0.1% (v/v) TFA, pH 2 at typical concentrations in the range of 12 to 32 μ M (monomer equivalents) were placed into 1 mm quartz cuvettes (Helma, Germany) and measured with following instrument settings on a Jasco J-1100 CD spectropolarimeter: 0.1 nm step size, 50 nm/min scan speed, 1 nm bandwidth, 10 accumulations, 20°C.

Rotor filling and pH shift

 $[U^{-13}C,^{15}N]$ -pEA β (3-42) fibrils in aqueous 30% (v/v) ACN, 0.1% (v/v) TFA, pH 2 were harvested by centrifugation (15.000 xg, 60 min) and applied by centrifugation (500 xg, 60 sec), into a 3.2 mm thick wall rotor (Bruker, Germany) by homemade rotor filling tools. For the pH 6.5 shifted fibril sample harvested [U-13C,15N]-pEAβ(3-42) fibrils (grown at pH 2 in 30% (v/v) ACN, 0.1% (v/v) TFA) were adjusted to pH 6.5 by addition and mixing of 10 µl citrate-phosphate buffer stock, pH 7.0 $^{[20]}$ to 40 μl harvested fibril pellet as described previously.[11] The citrate-phosphate buffer stock was obtained by mixing aqueous solutions of 17.65 vol % of 0.25 M citric acid and 82.35 vol % of 0.5 M Na₂HPO₄. The pH 6.5 adjusted [U- 13 C, 15 N]pEAβ(3-42) fibril sample thus contained aqueous 24% (v/v) ACN, $0.08\,\%$ (v/v) TFA, $82.35\,mM$ Na_2HPO_4 , $8.825\,mM$ citric acid, and placed in a 3.2 mm thin wall rotor (Bruker, Germany) as described above. As previously described for [U-¹³C, ¹⁵N]-Aβ(1-42) fibrils^[11] each 50 μ l rotor sample contains ~1.7 to 2.1 mg [U- 13 C, 15 N]-pEA β (3-42) fibrils, equivalent to 380 to 460 nmol monomer equivalents of $[U^{-13}C,^{15}N]$ -pEA β (3-42), which corresponds to final $[U^{-13}C,^{15}N]$ pEAβ(3-42) concentrations of 7.5 to 9.3 mM. Thus, the fibril preparations contain ~96% solvent and are highly hydrated. In our previous study on pH 2 to pH 7 adjusted A β (1-42) fibrils, we could exclude an effect of the citrate-phosphate buffer on the $A\beta(1-42)$ fibril structure.[11]

Solid-state NMR experiments

Solid-state NMR experiments were conducted on an 18.8 T (800 MHz ¹H frequency) Avance III and 14.1 T (600 MHz ¹H frequency) Bruker AVANCE NEO spectrometer equipped with triple resonance HCN 3.2 mm MAS Efree probes. Typical radiofrequency field strengths were 91-100 kHz for ¹H, 55.6 kHz for ¹³C and 45.5 kHz for ¹⁵N. The VT gas temperature was set to 263 K (thermocouple reported temperature); the sample temperature was estimated to be around 5-10 K higher due to frictional heating under MAS. Spinal $64^{[21]}$ ^{1}H decoupling (rf field of 85 kHz) was applied during ¹³C acquisition. The MAS frequency was set to 11 kHz for most of the Proton Driven Spin Diffusion (PDSD) and NCACX/NCOCX experiments, 12.5 kHz for other PDSD, 17.2 kHz for Rotational Resonance experiments and 20 kHz for Dipolar Assisted Rotational Resonance (DARR). Detailed experimental parameters can be found in Table S1. 13C chemical shifts were externally referenced using adamantane by setting its CH signal to 31.4 ppm (corresponding to the DSS reference scale). The ¹⁵N chemical shifts were indirectly referenced to liquid NH₃. All spectra were processed using TopSpin 3.5 and 4.0.9 (Bruker). The analysis was performed using CcpNMR Analysis 2.4.[22]

Water-edited experiments: To probe water-accessibility of the fibrils, we performed water-edited 1D experiments, where ¹H polarization of the protein is destroyed using a spin-echo T_2 -filter with a τ of 2.5 ms duration, followed by a transfer of ¹H polarization from water back onto the protein by longitudinal ¹H-¹H mixing^[23] (Figure S8A). Chemical exchange of protons as well as spin diffusion at the water-protein interface lead to higher intensities for waterexposed residues compared to residues in the dry interior of the protein.[24] For the global water accessibility, we integrated the aliphatic regions of the water-edited 1D ¹³C CP spectra for the pEA β (3-42) and A β (1-42) fibrils at pH 2 and pH 6.5 (Figure S8B, C). Comparing water build-up times, we observe a slower build-up for pEA β (3-42) than for A β (1-42) fibrils at both pH values of pH 2 and pH 6.5 (Figure S8D), which might be caused by the higher hydrophobicity, as three charges are missing for the shorter peptide. Additionally, the build-up is only slightly enhanced for pH 6.5 compared to pH 2 due to faster chemical exchange, [18] also indicating that the global structure is retained over ~five pH units.

Acknowledgements

The authors gratefully acknowledge experimental assistance by Robin Backer and Celina Schulz, Heinrich-Heine-Universität Düsseldorf (HHU). Access to the Jülich-Düsseldorf Biomolecular NMR Center jointly run by Forschungszentrum Jülich and HHU is acknowledged. HH was supported by the Entrepreneur Foundation at HHU and the DFG (HE 3243/4-1 and INST 208/771-1 FUGG). NMR data are deposited in the Biological Magnetic Resonance Data Bank (BMRB) under accession number 51993. Open Access funding enabled and organized by Projekt DEAL.

Conflict of Interests

The authors declare no conflict of interest.

Data Availability Statement

The data that support the findings of this study are openly available in BMRB at https://bmrb.io, reference number 51993.

Keywords: Amyloid beta-peptides · NMR spectroscopy · Neurodegenerative diseases · Alzheimer's disease · Pyroglutamate formation

- M. Hashimoto, E. Rockenstein, L. Crews, E. Masliah, NeuroMol. Med. 2003. 4, 21–36.
- [2] a) G. Bitan, M. D. Kirkitadze, A. Lomakin, S. S. Vollers, G. B. Benedek, D. B. Teplow, *Proc. Natl. Acad. Sci. USA* **2003**, *100*, 330–335; b) M. Folin, S. Baiguera, M. Tommasini, D. Guidolin, M. T. Conconi, E. De Carlo, G. G. Nussdorfer, P. P. Parnigotto, *Int. J. Mol. Med.* **2005**, *15*, 929–935; c) T. Iwatsubo, A. Odaka, N. Suzuki, H. Mizusawa, N. Nukina, Y. Ihara, *Neuron* **1994**, *13*, 45–53.
- [3] a) O. Wirths, S. Zampar, Expert Opin. Ther. Targets 2019, 23, 991–1004;
 b) M. Wulff, M. Baumann, A. Thummler, J. K. Yadav, L. Heinrich, U. Knupfer, D. Schlenzig, A. Schierhorn, J. U. Rahfeld, U. Horn, J. Balbach, H. U. Demuth, M. Fandrich, Angew. Chem. Int. Ed. Engl. 2016, 55, 5081–5084
- [4] a) M. P. Kummer, M. T. Heneka, Alzheimer's Res. Ther. 2014, 6, 28; b) S. Schilling, T. Hoffmann, S. Manhart, M. Hoffmann, H. U. Demuth, FEBS Lett. 2004, 563, 191–196.
- [5] a) O. Wirths, H. Breyhan, H. Cynis, S. Schilling, H. U. Demuth, T. A. Bayer, Acta Neuropathol. 2009, 118, 487–496; b) L. C. Camargo, M. Schoneck, N. Sangarapillai, D. Honold, N. J. Shah, K. J. Langen, D. Willbold, J. Kutzsche, S. Schemmert, A. Willuweit, Int. J. Mol. Sci. 2021, 22; c) T. Dunkelmann, S. Schemmert, D. Honold, K. Teichmann, E. Butzkuven, H. U. Demuth, N. J. Shah, K. J. Langen, J. Kutzsche, D. Willbold, A. Willuweit, J. Alzheimer's Dis. 2018, 63, 115–130.

- [6] C. Dammers, M. Schwarten, A. K. Buell, D. Willbold, Chem. Sci. 2017, 8, 4996–5004.
- [7] a) C. Dammers, L. Gremer, P. Neudecker, H. U. Demuth, M. Schwarten, D. Willbold, *PLoS One* 2015, 10, e0139710; b) C. Dammers, L. Gremer, K. Reiss, A. N. Klein, P. Neudecker, R. Hartmann, N. Sun, H. U. Demuth, M. Schwarten, D. Willbold, *PLoS One* 2015, 10, e0143647; c) C. Dammers, K. Reiss, L. Gremer, J. Lecher, T. Ziehm, M. Stoldt, M. Schwarten, D. Willbold, *Biophys. J.* 2017, 112, 1621–1633.
- [8] a) H. A. Scheidt, J. Adler, M. Krueger, D. Huster, Sci. Rep. 2016, 6, 33531;
 b) H. A. Scheidt, J. Adler, U. Zeitschel, C. Höfling, A. Korn, M. Krueger, S. Roßner, D. Huster, Chem. Eur. J. 2017, 23, 15834–15838.
- [9] a) Y. Xiao, B. Ma, D. McElheny, S. Parthasarathy, F. Long, M. Hoshi, R. Nussinov, Y. Ishii, Nat. Struct. Mol. Biol. 2015, 22, 499; b) M. T. Colvin, R. Silvers, Q. Z. Ni, T. V. Can, I. Sergeyev, M. Rosay, K. J. Donovan, B. Michael, J. Wall, S. Linse, R. G. Griffin, J. Am. Chem. Soc. 2016, 138, 9663–9674; c) M. A. Wälti, F. Ravotti, H. Arai, C. G. Glabe, J. S. Wall, A. Böckmann, P. Güntert, B. H. Meier, R. Riek, Proc. Natl. Acad. Sci. USA 2016, 113, E4976-E4984; d) A. Wickramasinghe, Y. Xiao, N. Kobayashi, S. Wang, K. P. Scherpelz, T. Yamazaki, S. C. Meredith, Y. Ishii, J. Am. Chem. Soc. 2021, 143, 11462–11472.
- [10] L. Gremer, D. Schölzel, C. Schenk, E. Reinartz, J. Labahn, R. B. G. Ravelli, M. Tusche, C. Lopez-Iglesias, W. Hoyer, H. Heise, D. Willbold, G. F. Schröder, Science 2017, 358, 116–119.
- [11] N. Becker, B. Frieg, L. Gremer, T. Kupreichyk, L. Gardon, P. Freiburg, P. Neudecker, D. Willbold, H. Gohlke, H. Heise, J. Am. Chem. Soc. 2023, 145, 2161–2169.
- [12] D. S. Wishart, B. D. Sykes, J. Biomol. NMR 1994, 4, 171–180.
- [13] O. C. Andronesi, S. Becker, K. Seidel, H. Heise, H. S. Young, M. Baldus, J. Am. Chem. Soc. 2005, 127, 12965–12974.
- [14] A. Hinterholzer, V. Stanojlovic, C. Cabrele, M. Schubert, *Anal. Chem.* 2019, 91, 14299–14305.
- [15] L. Siemons, B. Uluca-Yazgi, R. B. Pritchard, S. McCarthy, H. Heise, D. F. Hansen, Chem. Commun. (Camb.) 2019, 55, 14107–14110.
- [16] Y. Shen, A. Bax, J. Biomol. NMR 2013, 56, 227-241.
- [17] a) F. Creuzet, A. McDermott, R. Gebhard, K. van der Hoef, M. B. Spijker-Assink, J. Herzfeld, J. Lugtenburg, M. H. Levitt, R. G. Griffin, Science 1991, 251, 783–786; b) T. G. Oas, R. G. Griffin, M. H. Levitt, J. Chem. Phys. 1988, 89, 692–695.
- [18] V. S. Mandala, A. R. Loftis, A. A. Shcherbakov, B. L. Pentelute, M. Hong, Nat. Struct. Mol. Biol. 2020, 27, 160–167.
- [19] D. Necas, P. Klapetek, Cent. Eur. J. Phys. 2012, 10, 181–188.
- [20] T. C. McIlvaine, J. Biol. Chem. 1921, 49, 183-186.
- [21] B. M. Fung, A. K. Khitrin, K. Ermolaev, J. Magn. Reson. 2000, 142, 97–101.
- [22] W. F. Vranken, W. Boucher, T. J. Stevens, R. H. Fogh, A. Pajon, M. Llinas, E. L. Ulrich, J. L. Markley, J. Ionides, E. D. Laue, *Proteins* 2005, 59, 687–696.
- [23] a) A. Lesage, A. Bockmann, J. Am. Chem. Soc. 2003, 125, 13336–13337;
 b) C. Ader, R. Schneider, K. Seidel, M. Etzkorn, S. Becker, M. Baldus, J. Am. Chem. Soc. 2009, 131, 170–176;
 c) J. K. Williams, M. Hong, J. Magn. Reson. 2014, 247, 118–127.
- [24] M. D. Gelenter, K. J. Smith, S.-Y. Liao, V. S. Mandala, A. J. Dregni, M. S. Lamm, Y. Tian, W. Xu, D. J. Pochan, T. J. Tucker, Y. Su, M. Hong, *Nat. Struct. Mol. Biol.* 2019, 26, 592–598.

Manuscript received: November 20, 2023 Accepted manuscript online: December 15, 2023 Version of record online: December 29, 2023